Mathematical Modeling Of The Mononitride Nuclear Fuel Production Processes

I.V.Peshkichev[1],   I.R.Makeyeva[1],   V.A.Simoneko[1],   O.V.Shults[1],   A.A.Bochkareva[1],
V.G.Dubosarskiy[1],   V.Yu.Pugachev[1],   O.V.Kuznetsova[1],   L.N.Darina[1],   N.Yu.Romanova[1],
A.E.Paukova[1]

[1]Russian Federal Nuclear Center - Zababakhin All-Russian Scientific Research Institute of Technical Physics

E-mail contact of main author: I.V.Peshkichev@vniitf.ru

Abstract. The paper describes mathematical models for basic processes of mixed nitride uranium-plutonium fuel fabrication: carbothermic synthesis, pressing of powder into pellets, and sintering of pellets. Calculations for general properties of the products depending on the starting material features and process conditions were carried out using the developed mathematical models. Appropriate examples are given.

Key Words: mathematical modeling, carbothermic synthesis, pressing, sintering.

1. Introduction

Implementation program of fast neutron reactors in nuclear power engineering involves new types of nuclear fuel, specifically nitride. RFNC-VNIITF in cooperation with VNIINM develops models and codes for simulation of physical and chemical processes of production of mixed nitride uranium-plutonium fuel. The purpose of this work is mathematical support for development and implementation of fabrication technique for mixed nitride uranium-plutonium fuel. The main objective is to create the software that enables one to select and optimize the process conditions.

The fabrication technique for mixed nitride uranium-plutonium fuel involves the following processes:

—   Carbothermic synthesis suggests that uranium oxide and plutonium oxide powders mixed with graphite are treated at high temperature in the nitrogen flow. Strict requirements in relation to the residual oxygen and carbon contents are applied to the end product obtained during this process. Mathematical simulation is hindered by an uninvestigated staged reaction mechanism. The overall reaction appears as $(U, Pu)O_2 + 2C + 0,5N_2 = (U, Pu)N + 2CO$.

—   Crushing and mixing of powders is used to attain appropriate particle size distribution and homogenization of mixture.

—   Granulation implies mixing the powders having an organic bond, pre-compaction and milling before pressing. This process is used to ensure the original powder yield and constant bulk weight necessary for uniform dosing and filling of the product into the mold of an automatic press. Together with crushing, it is the simplest and most efficient operation.

—   Pressing is the process of fuel pellet forming in automatic press. Interaction of pressing material with the punch and the mold material may result in nonuniformly distributed density throughout the pellet, which may lead to spallation and fracture of pellets

during sintering. Thus, the following set of process parameters is to be considered: pressure, loading time, loading rate and knockout, mechanical and rheological properties of the powder, composition and amount of applied binding agent, shape and size-distribution of the particles.

—   Sintering is the main procedure in the fuel fabrication process. It is necessary for the pellet to attain the required density and mechanical strength. During sintering, the porosity is decreasing, thus leading to shrinkage of the pellet and growth of grains. Nitride dissociation at high temperatures is one of the key problems.

Mathematical models are developed for the mentioned processes. The models are implemented as program codes designed to compute the principal properties of the products depending on the starting material features and process conditions. This paper presents the mathematical models for carbothermic synthesis, pressing and sintering, simulation results.

2.   Nitride Fuel Carbothermic Synthesis

VNIINM provided for the data, which was used as the initial data to develop the model. The data comprises records of the mass-spectrometer used to analyze the gaseous phase composition at the outlet of the system for carbothermic synthesis, as well as the data for the synthesis conditions, the initial and finite elemental composition. The synthesis was carried in the following manner: heating in N_2- atmosphere up to 1580 °C (for 3.2 hours), soaking (for 9 hours), replacing with N_2-H_2 atmosphere and soaking at 1540 °C (for 31.4 hours), cooling in Ar (for 2 hours). Figure 1 shows the ion current records for mass-to-charge ratios 2, 12, 14, 16, and 40 (atomic mass unit/elementary charge) that are roughly corresponding to the ions $^{1}H_2^{+}$, $^{12}C^{+}$, $^{14}N^{+}$, $^{16}O^{+}$, $^{40}Ar^{+}$.
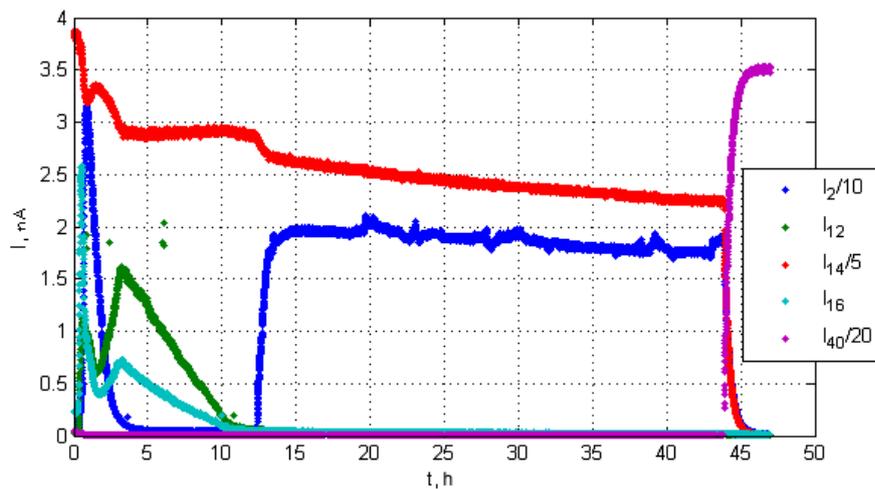

Figure 1. Mass-spectrometer records

To analyze the carbothermic synthesis kinetics we proceed from the assumption that an ion current for the mass-to-charge ration equal to 12 corresponds to $^{12}C^{+}$ ions evolving from CO molecules. Hence the ion current value is proportional to CO escaping from the reactor. When taken into account that the reactor is flow reactor and the gas flow is maintained at nearly the same level, it follows that CO concentration at the reactor outlet is proportional to the total reaction rate, thus the ion current versus time curve recorded by the mass-spectrometer can be used to track the overall reaction rate.

To determine the value of the ion current integral, the recorded curve was split into three stages (Figure 2):
—   Stage 1 – starting from the curve recording until the moment 3.1 hours;

—— Stage 2 – from the moment 3.1 to 10 hours;
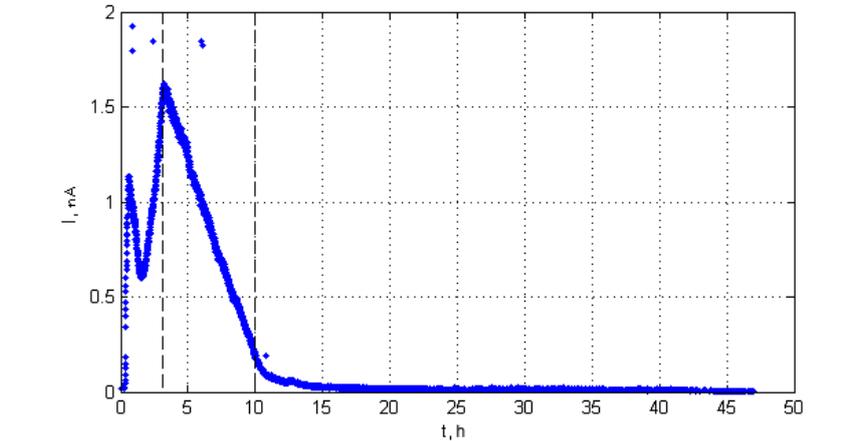—— Stage 3 – from 10 hours to completion of the curve recording.

Figure 2. Ion current for the mass-to-charge ratio equal to 12

At each stage, the curve was approximated by the following equations:

—— Stage 1 – $I_{12} = \exp(a_1 \cdot t + b_1)$;

—— Stage 2 – $I_{12} = a_2 \cdot t + b_2$;

—— Stage 3 – $I_{12} = \dfrac{1}{a_3 \cdot t + b_3}$.

The obtained coefficients of regression equations were used to calculate the ion current integral taken over the time – the total charge. The factor of proportionality between the current and the reaction rate was derived. The coefficient value and the obtained regressions were used to calculate amounts of the residual carbon in the mixture as a factor of time. Figure 3 shows the calculation data.
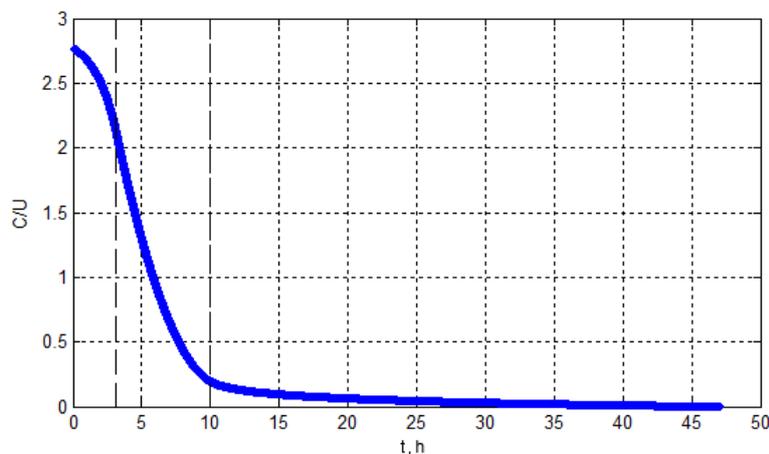

Figure 3. Carbon amounts in the mixture per unit of uranium as a function of time

To find the reaction rate constant, an assumption is made that the reaction is of the first order. In this case, the kinetic equation takes the following form:

$$-\ln\left(1 - \frac{x}{n_0}\right) = k \cdot t$$

,   (1)

where x is the reacted material quantity, mole; n_0 – the material substance initial quantity, mole; k – rate constant, s^{-1}; t – time , s.

The rate constant is determined by the slope of the curve for the reacted carbon quantity as a function of time in the coordinates $\ln(1-x/C_0) - t$. Figure 4 shows this dependence for the second stage.
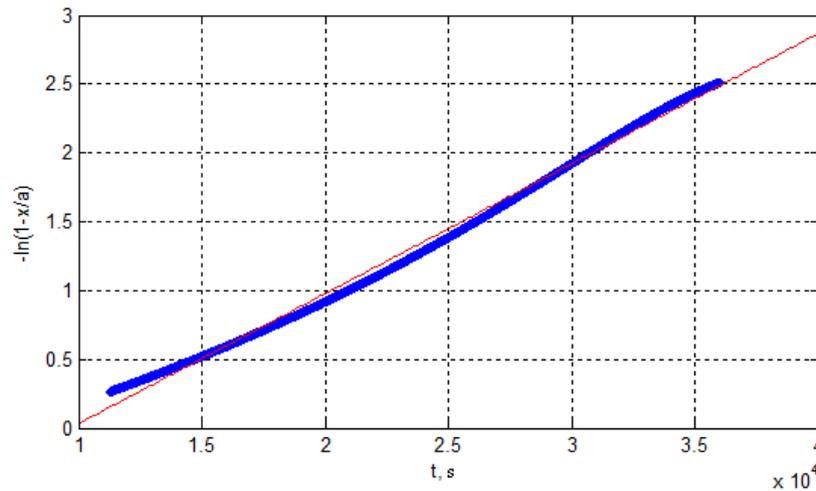

Figure 4. Reacted carbon amount as a function of time:
The blue line indicates experimental data, the red line – the linear approximation

In accordance with the approximating dependence derived, the process rate constant at 1580 °C equals to $9.446 \cdot 10^{-5}$ s^{-1}.

The initial quantities of oxides and carbon in the mixture, temperature and process time were used as the initial data to carry out calculations. The overall reaction equation and the data for the initial quantities of oxides and carbon in the mixture are used to determine, which of the components is in excess and which one is in deficiency. The formula below is used to determine the amount of an insufficient component n for the moment of time t:

$$n = n_0 \cdot \exp\left[-\int_0^t k dt\right],$$

(2)

where n is the amount of the remaining substance material, mole for the moment of time t, s; n_0 is the initial amount of the substance material, mole; k is the rate constant, s^{-1}.

The quantities of the remaining components are determined according to the stoichiometric coefficients of the overall reaction equation. Considering that at stage 3, hydrogen is added in the atmosphere, the relation between carbon quantities escaping the furnace and the degree of advancement of the reaction changes, thus the approach outlined above can be only applied during the first two stages of the process. To describe completeness of the entire process, it is also necessary to consider kinetics of the residual carbon elimination in the presence of hydrogen.

The element composition of the system is determined by simulation.

The described model can be applied to calculate the powder composition dependence on time for the initial conditions and the temperature-time relationship corresponding to the experiment. Figure 5 shows the resultant dependence.
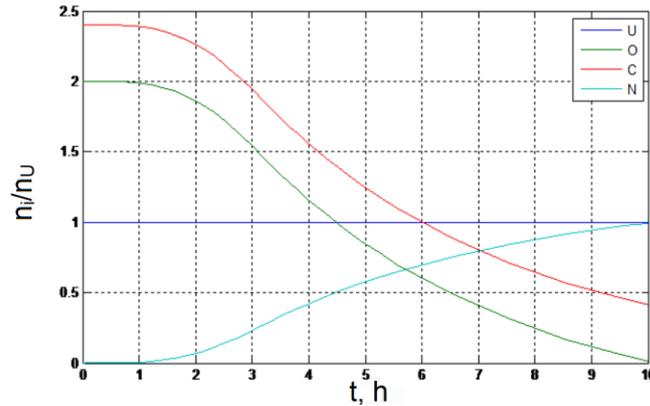
Figure 5. Amount of matter in the mixture per unit of uranium versus time curve

The calculation results are in good agreement with the data deduced from the mass-spectrometry analysis of a gaseous fluid escaping from the reaction zone in the process of uranium and plutonium mononitride synthesis at VNIINM laboratory. The developed model allows calculating the powder composition versus the synthesis time without recourse to the parameters requiring additional experiments.

3. Mathematical Model for Pressing

The finite-element method is used to develop the mathematical model for pressing of fuel pellets. The basic idea of the method suggests that any continuous value like temperature, pressure and motion (transfer) can be approximated by a discrete model, which is constructed using a set of piecewise continuous functions estimated by a finite number of subregions [1]. The finite-element model, which was used in the calculations, is axisymmetric. It was developed from the four-node axisymmetric elements. Figure 6 shows the model.

Presence of the symmetry plane, due to double-sided pellet pressing, was used to develop the model. The pellet height was taken as 10 mm, the diameter was 9.05 mm. The interaction between the pellet, the punch and the matrix (mold) is simulated by contact elements, the friction factor on the surface contact area was taken as equal to f = 0.1.

Loading was given as downward motion of the punch, the distance of movement was equal to half of the initial height of the pellet.
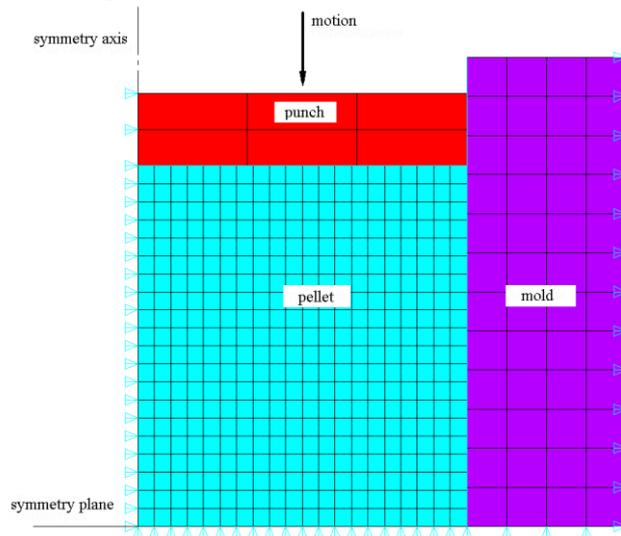

Figure 6. Finite-element model

A bilinear plastic material model was used for the pellet. The model had the following properties: elastic module E = 500 MPa; Poisson's ratio μ = 0.05; yield point σ_T = 100 MPa, and hardening module E_{elas} = 500 MPa. The creep strain was described using the following law:

$$\xi = C_1 \exp\left(\frac{\sigma}{C_2} - \frac{C_3}{T} \right) \tag{3}$$

where C_1, C_2, C_3 are creep coefficients; $C_1 = 1 \cdot 10^{13}$ s^{-1}; $C_2 = 0.5$ MPa; $C_3 = 2 \cdot 10^4$ K; T – temperature.

The matrix (mold) material was steel. It offered the following properties: E = $2 \cdot 10^5$ MPa, μ = 0.3. To eliminate noticeable deformation of the punch, the material was taken as very stiff. It also possessed the following properties: E = $2 \cdot 10^9$ MPa, μ = 0.3. The calculations simulated increased loading (motion) and holding under stress. The load rise time was set as 10 seconds, the holding time lasted for 90 seconds, total loading time was 100 seconds. An option of large deformation was used in computing because the pellet is severely deformed at pressing. While in pressing, the temperature of pellets was taken as 40 °C.

The calculation data demonstrated non-uniform compression of the pellets. Figure 7 shows distribution of vertical displacements over the pellet cross-section. The figure shows that the displacement over the matrix (mold) walls is lower than in the central zone, which is explained by the friction force. The calculations also demonstrated the presence of radial displacements in the pellet during pressing. Figure 8 shows distribution of radial displacements, the pellet layers adjacent to the punch had radial displacements towards the pellet center, and the layers of the pellet adjacent to the symmetry plane, had radial displacements outwards the pellet center. Such radial displacements of the layers are due to deceleration of vertical displacements over the matrix (mold) walls.
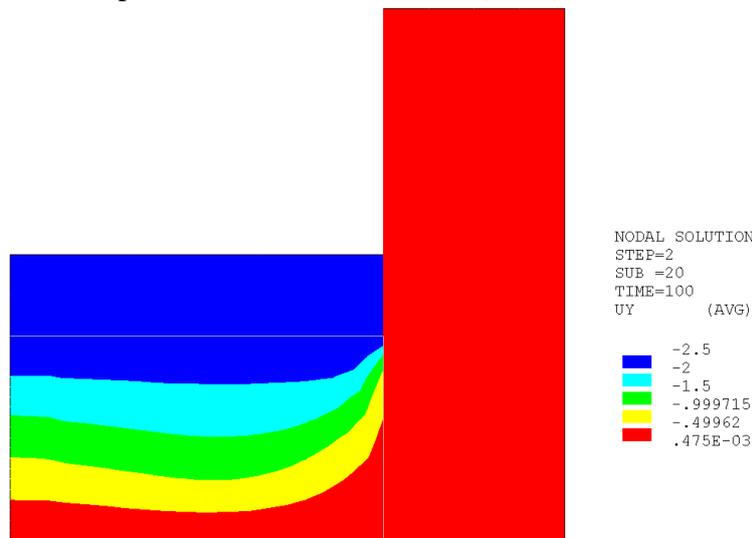

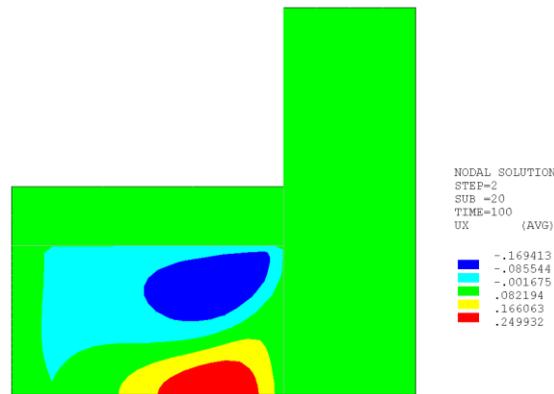*Figure 7. Distribution of vertical displacements over the pellet cross-section, mm*

Figure 8. Distribution of radial displacements over the pellet cross-section, mm

The calculation showed that the results are markedly affected by the friction factor value. Figure 9 demonstrates the distribution of vertical displacements over the pellet cross-section for an increased value of the friction factor f = 0.15. The displacement distribution pattern turned out to be similar to the distribution for the initial friction factor value but the difference between the displacements over the matrix (mold) walls and displacements in the central zone increased.
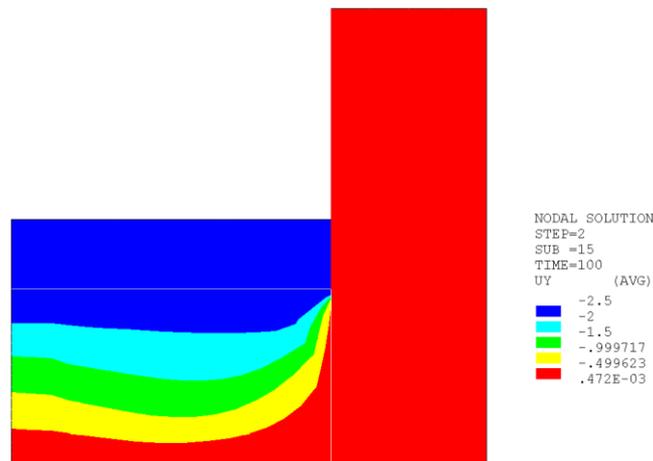

Figure 9. Distribution of vertical displacements over the pellet cross-section for the increased friction factor value, mm

The developed model makes it possible to calculate the distribution of vertical and radial displacements, bulk and contact pressure as well as to estimate the effects of the friction factor and elasticity module on vertical displacements in the pellet and the punch force.

4. Model for Nitride-Uranium Sintering

Approximating approach was proposed as a basis for development of nitride-uranium sintering model. The experimental data reported in [2] was used as the initial data for simulation. The data refers to the finite-density dependencies of the sintered sample on the sintering temperature and the sintering atmosphere at similar original parameters of pressed samples.

All in all, the paper presents three sets of sintering conditions:
— Sintering at high nitrogen pressure (1140 torr);
— Sintering at low nitrogen pressure (0.1 torr);

— Sintering in argon atmosphere under the pressure 1140 torr with addition of nitrogen (partial nitrogen pressure makes 0.1 torr).

The paper shows that two of the last mentioned variations of atmosphere provided a similar result, so they were combined to make one group. Hence the nitride-uranium sintering experiments at low nitrogen pressure (also mixed with argon) and experiments at high nitrogen pressure were considered.

The initial state of the compacts was taken as appropriate to the particle distribution of the initial powder, which was described in paper [2]. In addition, the temperature-time conditions of sintering also corresponded to the conditions implemented in the experiments and incorporated the following stages:

— Heating from temperature 1300 °C up to the operation temperature for 15 minutes;
— Holding at the operation temperature for 2 hours;
— Cooling from the operation temperature up to 1100 °C for 15 minutes.

Series of calculations for high and low nitrogen pressure were carried out using the above-mentioned initial data and conditions of the sintering process. The model parameters i.e. activation energy and pre-exponential factor varied in the calculations. These parameter values were finally obtained: for a series of experiments at low nitrogen pressure, the activation energy amounted to 100 kJ/mole, pre-exponential factor amounted to $9.98 \cdot 10^{-44}$ m^{11}/s; for a series of experiments at high nitrogen pressure were 220 kJ/mole and $4.19 \cdot 10^{-41}$ m^{11}/s respectively. The activation energy of the uranium nitride sintering based on Debay temperature correlation made 284 kJ/mole, 29% more than the value obtained in the present paper (corresponding to sintering at high nitrogen pressure). Figure 10 show the results of experiments and calculations at these parameter values for low nitrogen pressures.
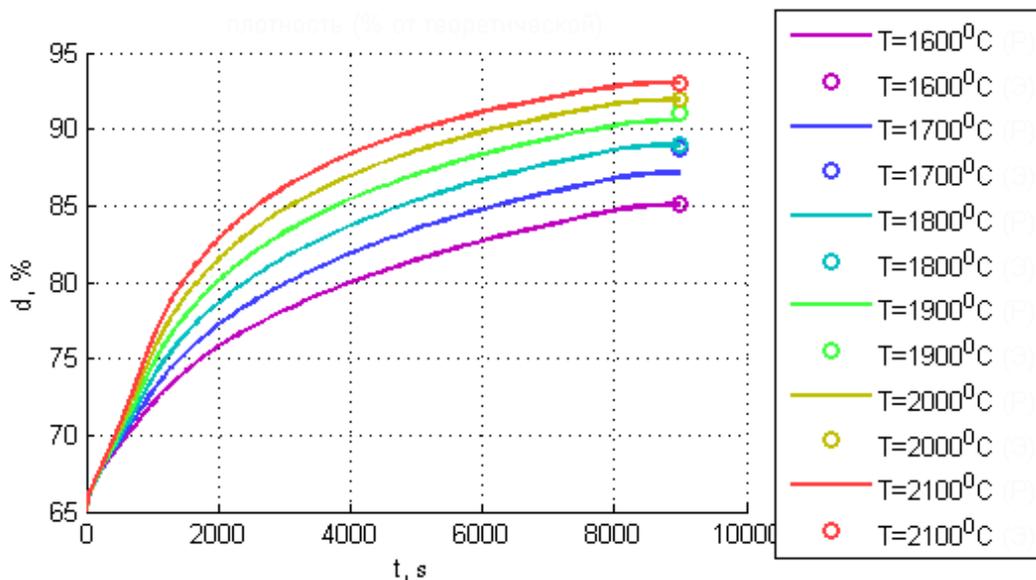

Figure 10. Density (% from apparent density) versus holding time (s) curve. Results of calculations (lines) and experiments (markers) for UN sintering at low nitrogen pressure. The legend indicates the operating temperatures of sintering

From figure 10 we notice that the calculation results at chosen values of constants are in good agreement with the results of experiments.

The obtained parameter values of the model were used to calculate the sintering process pattern diagram for low and high nitrogen pressure. The pattern diagrams show association of the sintered sample finite density with the temperature and holding time. Heating time up to the operating temperature and cooling time are set similar to the conditions discussed above – 15 minutes each.
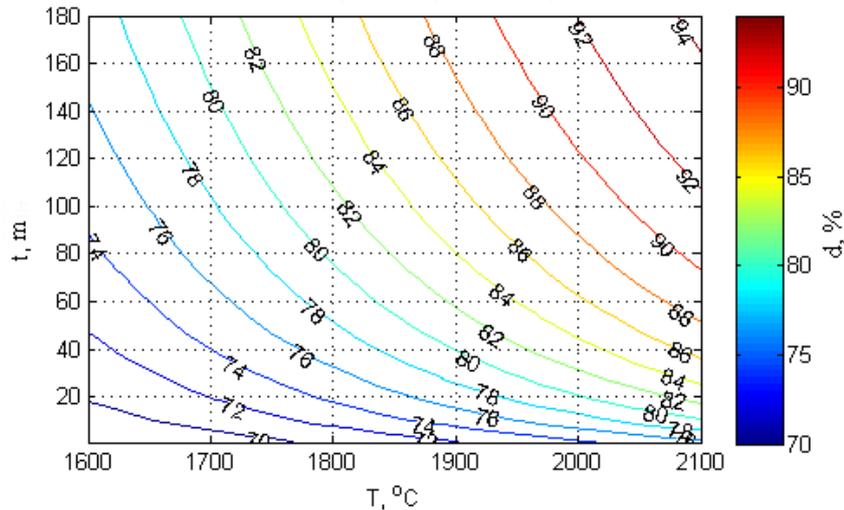

Figure 11. Pattern diagrams for uranium nitride sintering at high nitrogen pressure. Density (% from apparent density) versus holding time (m) and temperature (°C)
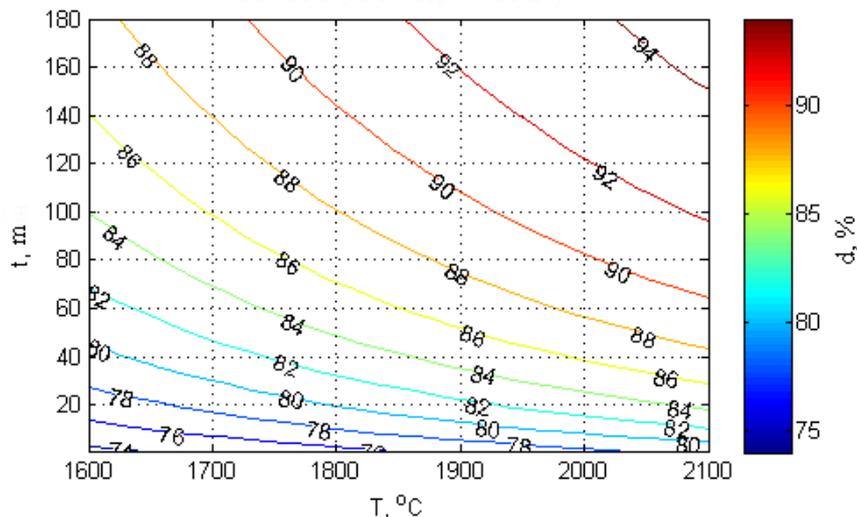

Figure 12. Pattern diagrams for uranium nitride sintering at low nitrogen pressure. Density (% from apparent density) versus holding time (m) and temperature (°C)

Figures 11 and 12 show the pattern diagrams for uranium nitride sintering at high and low nitrogen pressure, respectively. From these figures we notice that at low nitrogen pressure, higher density is reached at lower temperatures and less holding time as compared to higher nitrogen pressure.

The sintering model permits calculation of density variation, as well as temporal variations for linear dimensions of the material versus temperature-time conditions of sintering. Calculations based on these models make possible selection of an optimum sintering mode for the designated end density of the material. Use of the models in sintering of mixed nitride uranium-plutonium fuel requires determination of the specified material constants in the course of experiments.

5. Conclusion

This paper describes mathematical models for principal processes within the fabrication technology for mixed nitride uranium-plutonium fuel developed at RFNC-VNIITF in cooperation with VNIINM.

Model for carbothermic synthesis. The data for mass-spectrometry analysis of gaseous products of carbothermic synthesis has been processed. The kinetic process parameters for heating stages and isothermal holding are obtained by processing taking into account an assumption that nitride reaction is of the first order. The resulting composition algorithm depending on the initial composition and the temperature-time conditions of the process has been suggested. The described model was used to calculate the product composition dependence on time.

Model for pressing The finite-element method was used to implement the model. The model allows calculation of vertical and radial displacements, bulk and contact pressure as well as punch force. Mechanical properties of the pellet, die-mold and punch: friction factor, elasticity module, yield stress and strengthening module are taken into account. Such calculations can be applied to determine the possibility for initiation of defects in the pellet. The calculation results can be represented as a measurement variable gradient over the pellet cross-section. The model was used to estimate the effect of friction factors and elasticity module on vertical displacements in the pellet and the punch force. To use the model in calculations of particular powders pressing process, physical and mechanical properties of the materials, which can be produced as a result of the experimental program, are required.

Model for sintering. The model permits calculation of density variation and changes of the material linear dimensions as a function of temperature and time conditions of sintering. The developed model was used to calculate the sintering diagram patterns for two cases - high and low nitrogen pressure. The patterns demonstrate the interrelation between the temperature and time of isothermal holding and the relative density of sintered pellets.

The set of developed models is intended for calculation of main properties of the products versus the properties of the starting material and process conditions. An experimental program has been prepared to verify the models. The models are used to write the software that can be used to select and improve the processing conditions for mixed nitride uranium-plutonium fuel production technology.

<div align="center">REFERENCES</div>

[1]   LEVIN, V.A., VERSHININ, A.V., Nonlinear computational density mechanics. V. 2 Numerical methods. Parallel computer calculations, Fizmatlit, Moscow (2015) (in Russian).

[2]   TENNERY V.J., GODFREY T.G., POTTER R.A., Sintering of UN as a Function of Temperature and N2 Pressure, Journal of The American Ceramic Society, Vol. 54, No.7, pp. 327-331, (1971).